Applied Physics Letters

Tunable thermal expansion and magnetism in Zr-doped ScF_3

Cite as: Appl. Phys. Lett. **109**, 181901 (2016); https://doi.org/10.1063/1.4966958
Submitted: 17 August 2016 . Accepted: 16 October 2016 . Published Online: 02 November 2016

Tao Wang, Jiale Xu, Lei Hu, Wei Wang, Rongjin Huang, Fei Han, Zhao Pan, Jinxia Deng, Yang Ren, Laifeng Li, Jun Chen, and Xianran Xing

Tunable thermal expansion and magnetism in Zr-doped ScF_3

Tao Wang,[1] Jiale Xu,[1] Lei Hu,[1] Wei Wang,[2] Rongjin Huang,[2] Fei Han,[1] Zhao Pan,[1] Jinxia Deng,[1] Yang Ren,[3] Laifeng Li,[2] Jun Chen,[1,a)] and Xianran Xing[1,a)]
[1]*Department of Physical Chemistry, University of Science and Technology Beijing, Beijing 100083, China*
[2]*Key Laboratory of Cryogenics, Technical Institute of Physics and Chemistry, Chinese Academy of Sciences, Beijing 100190, China*
[3]*Argonne National Laboratory, X-Ray Science Division, Argonne, Illinois 60439, USA*

(Received 17 August 2016; accepted 16 October 2016; published online 2 November 2016)

The negative thermal expansion (NTE) behavior provides us an opportunity to design materials with controllable coefficient of thermal expansion (CTE). In this letter, we report a tunable isotropic thermal expansion in the cubic $(Sc_{1-x}Zr_x)F_{3+\delta}$ over a wide temperature and CTE range ($\alpha_l = -4.0$ to$+16.8 \times 10^{-6}$ K^{-1}, 298–648 K). The thermal expansion can be well adjusted from strong negative to zero, and finally to large positive. Intriguingly, isotropic zero thermal expansion ($\alpha_l = 2.6 \times 10^{-7}$ K^{-1}, 298–648 K) has been observed in the composition of $(Sc_{0.8}Zr_{0.2})F_{3+\delta}$. The controllable thermal expansion in $(Sc_{1-x}Zr_x)F_{3+\delta}$ is correlated to the local structural distortion. Interestingly, the ordered magnetic behavior has been found in the zero thermal expansion compound of $(Sc_{0.8}Zr_{0.2})F_{3+\delta}$ at room temperature, which presumably correlates with the unpaired electron of the lower chemical valence of Zr cation. The present study provides a useful reference to control the thermal expansion and explore the multi-functionalization for NTE materials. *Published by AIP Publishing*. [http://dx.doi.org/10.1063/1.4966958]

Most materials intrinsically expand upon heating, exhibiting positive thermal expansion. In contrast, a limited number of materials contract with increasing temperature, which is well known as the negative thermal expansion (NTE). NTE materials have significant applications in a variety of industrial fields, since they could be utilized to tailor the coefficient of thermal expansion (CTE) of components or devices.[1,2] Specially, isotropic zero thermal expansion (ZTE) materials are preferable because they can avoid thermal shock when subjected to a large temperature fluctuation. NTE behavior is intriguing yet complicated, since it generally entangles with lots of factors, such as spontaneous volume ferroelectrostriction in $PbTiO_3$-based ferroelectrics,[3] magnetovolume effect in Invar alloys[4] and antiperovskites,[5] charge-transfer in $BiNiO_3$,[6] and phonon-driven contraction in framework oxides,[7,8] fluorides,[9,10] zeolites,[11] metal organic frameworks (MOFs),[12] and Prussian Blue family.[13] In light of these complex mechanisms, the design of controllable NTE, or even the interesting isotropic ZTE, remains a challenge.

Recently, ScF_3 was reported to exhibit a striking NTE characteristic ($\alpha_l = -14 \times 10^{-6}$ K^{-1}, 60–110 K) and its CTE stays negative up to 1100 K without any phase transition.[9] Many attempts have been put to tune the CTE of ScF_3 by chemical substitution, such as the solid solution of $(Sc_{1-x}M_x)F_3$ (M = Al, Ti, and Y).[14–16] Some recent theoretical studies raise that the mismatch ionic radius between Sc^{3+} and other doping M^{3+} may weaken the NTE.[17] The substitution for Sc with similar size atoms induces less local structure distortions, which would give rise to large limit solubility of ScF_3-based solid solutions. Consequently, the smaller size mismatch between Sc^{3+} and M cations may be critical to achieve tunable thermal expansion in a wide temperature and CTE range. Herein, we introduce Zr^{4+} into ScF_3 to form a solid solution of $(Sc_{1-x}Zr_x)F_{3+\delta}$ due to the fact that Zr^{4+} (0.72 Å) has a similar ionic radius with that of Sc^{3+} (0.745 Å).[18] This chemical modification can bring a large solubility ($x \leq 0.7$) but still maintain the macroscopic cubic symmetry. Interestingly, the controllable thermal expansion from strong NTE to PTE has been achieved. The isotropic ZTE of $(Sc_{0.8}Zr_{0.2})F_{3+\delta}$ has been observed over a wide temperature range. Furthermore, room temperature magnetic order has been found in the ZTE composition of $(Sc_{0.8}Zr_{0.2})F_{3+\delta}$, while both ScF_3 and ZrF_4 exhibit diamagnetism. The present work not only broadens the scope of ZTE materials but also combines properties of NTE and magnetic order, which would provide a way to design multifunctional materials.

The solid solution of $(Sc_{1-x}Zr_x)F_{3+\delta}$ ($x = 0$–0.7) with various compositions has been prepared by a conventional solid-state reaction method. The lattice constant of cubic $(Sc_{0.8}Zr_{0.2})F_{3+\delta}$ has been calculated by Le Bail refinement method (Figure 1(a)). All the samples with different compositions remain the cubic structure (space group, $Pm\bar{3}m$) (Figure S1). For the composition of $(Sc_{0.3}Zr_{0.7})F_{3+\delta}$, some additional tiny peaks appear, which can be assigned to the peaks of ZrF_4 (I2/a, monoclinic). It means that the solid solubility limit of $(Sc_{1-x}Zr_x)F_{3+\delta}$ is around $x = 0.7$. With an increasing content of Zr, the lattice constant decreases linearly (Figure 1(b)), which can be directly indicated by the shift of (1 0 0) peaks from the lower 2θ region to the higher one (the inset of Figure 1(b)). The decrease in the lattice constant can be attributed to the introduction of the smaller radius of Zr cation (0.72 Å) compared with that of the Sc cation (0.745 Å). Furthermore, the linear contraction of lattice constant as a function of Zr content implies that the dopant of Zr cation occupies the site of Sc cation, which is consistent with the Vegard's law.[19]

In order to study the thermal expansion property, temperature dependence of XRD patterns have been performed for

a)Authors to whom correspondence should be addressed. Electronic addresses: junchen@ustb.edu.cn or xing@ustb.edu.cn. Tel./Fax:+86-10-82375027.

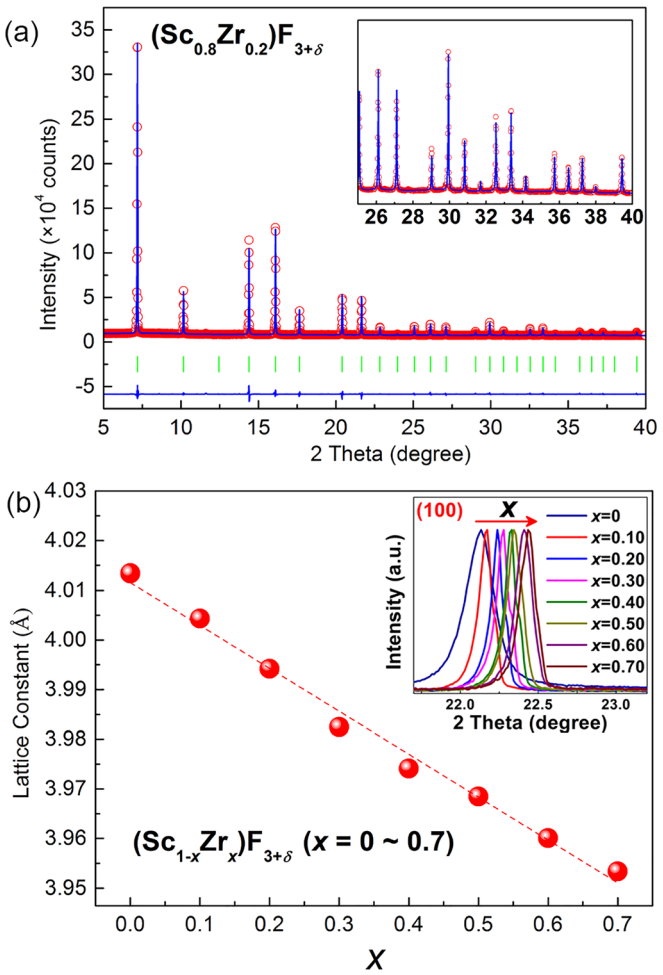

FIG. 1. (a) Le Bail fit of high resolution synchrotron X-ray diffraction data of $(Sc_{0.8}Zr_{0.2})F_{3+\delta}$ at room temperature. Observed (red circle) and calculated (blue line) data is presented. The green vertical bars show the reflection positions, and the blue solid line at bottom exhibits the difference profile. (b) Lattice constant a of $(Sc_{1-x}Zr_x)F_{3+\delta}$ ($x = 0$–0.7). The inset shows the (100) peaks of $(Sc_{1-x}Zr_x)F_{3+\delta}$ ($x = 0$–0.7).

the compositions of $(Sc_{1-x}Zr_x)F_{3+\delta}$ ($x = 0$–0.6). In the whole temperature range from 298 K to 648 K, all samples remain to be of the same cubic structure, and no phase transition occurs. The temperature dependence of $\triangle a$ ($a_T - a_{298K}$) is presented in Figure 2, in which the lattice constant was calculated from the Le Bail fitting. It is interesting to obtain that the linear CTE of $(Sc_{1-x}Zr_x)F_{3+\delta}$ can be adjusted from the strong NTE to ZTE and finally to large PTE (Figure 2). ScF_3 exhibits a smooth NTE behavior with a linear CTE of $\alpha_l = -4.0 \times 10^{-6}\,K^{-1}$ (298–648 K), consistent with the previous report.[20] It is interesting to note that the isotropic ZTE has been achieved in the composition of $(Sc_{0.8}Zr_{0.2})F_{3+\delta}$ ($\alpha_l = 2.6 \times 10^{-7}\,K^{-1}$, 298–648 K). With increasing substituted content of Zr, the NTE completely disappears and transforms into a strong PTE in the composition of $(Sc_{0.4}Zr_{0.6})F_{3+\delta}$ ($\alpha_l = +16.8 \times 10^{-6}\,K^{-1}$, 298–648 K).

The evolution of thermal expansion in the present system of $(Sc_{1-x}Zr_x)F_{3+\delta}$ could be correlated with the local distortion, which is introduced by the substitution of Zr in the macroscopic cubic lattice. The mismatch of the radii of Sc and Zr atoms could introduce the local distortion, the transverse thermal vibration of fluorine atoms would be reduced, and thus NTE is weakened.[20] Here, the local structural distortion of $(Sc_{0.8}Zr_{0.2})F_{3+\delta}$ is confirmed by the investigation of synchrotron X-ray total scattering of pair distribution function (PDF). As shown in Figure S3, even though $(Sc_{0.8}Zr_{0.2})F_{3+\delta}$ exhibits macroscopic cubic phase which is revealed by the XRD results, its local structure is distorted in rhombohedral one. The similar phenomena have also been reported in the previous work.[21] The transformation from NTE to ZTE, and finally to PTE is well correlated to the magnitude of local distortion.[21] When the local distortion is suitable, ZTE can be achieved such as in the present $(Sc_{0.8}Zr_{0.2})F_{3+\delta}$. With further increasing distortion, CTE will be modulated to be positive. Another effect for the considerable wide tunable CTE range would be attributed to the high solubility limit of Zr cations in the cubic $(Sc_{1-x}Zr_x)F_{3+\delta}$ ($x = 0$–0.6) solid solutions.

In addition to the controllable thermal expansion in $(Sc_{1-x}Zr_x)F_{3+\delta}$, the ferromagnetic order has also been observed in $(Sc_{0.8}Zr_{0.2})F_{3+\delta}$. Figure 3 shows the magnetic moment-field (M-H) plots at an ambient condition for $(Sc_{0.8}Zr_{0.2})F_{3+\delta}$. The ferromagnetic hysteresis loop can be clearly seen, and the coercivity is approximate 150 Oe (the inset at the bottom right of Figure 3). It is well known that

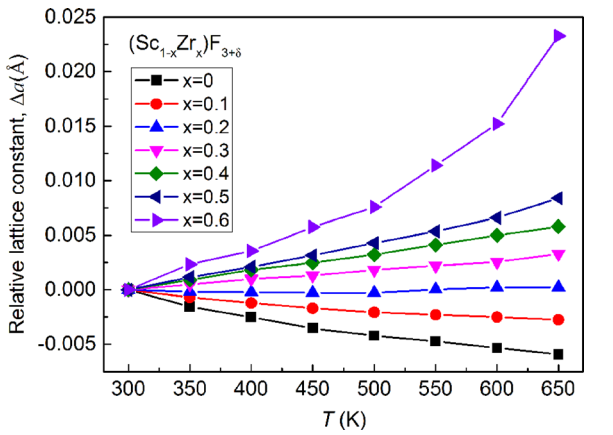

FIG. 2. The temperature dependence of the relative lattice constant, Δa ($a_T - a_{298K}$), of $(Sc_{1-x}Zr_x)F_{3+\delta}$ ($x = 0$–0.6).

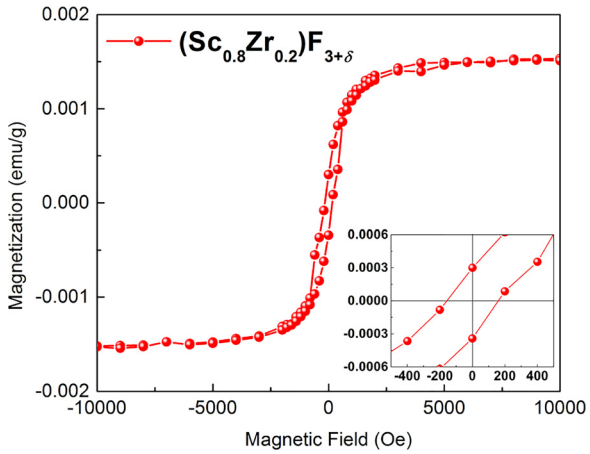

FIG. 3. M-H curve of $(Sc_{0.8}Zr_{0.2})F_{3+\delta}$ measured in an external magnetic field up to 10 kOe at room temperature. The inset displays H_c in the low magnetic region. The diamagnetic sign of the sample holder has been deducted.

ScF_3 exhibits a diamagnetic characteristic for its $3d^0$ electron configuration of the Sc^{3+} cation.[22] However, the ferromagnetic order is introduced by the substitution of Zr to Sc, which may be correlated with the lower chemical valence state of Zr cations.

In order to elucidate the possible origin of the ferromagnetic order, X-ray photoelectron spectra (XPS) have been performed to investigate the chemical valence state for Sc, Zr, and F ions. The XPS spectra of Sc 2*p* and F 1*s* are shown in Figures S5(a) and S5(b). Since the XPS peak of Sc 2*p* of $(Sc_{1-x}Zr_x)F_{3+\delta}$ is the same with that of the pure ScF_3, we can exclude the influence of Sc cations to the magnetic property. As seen in Figure 4, the area of Zr 3*d* peaks locating around the lower binding energy region in the two samples increases apparently when compared to that of the pure ZrF_4 (Figure S5(c)). The result may be ascribed to the emergence of the lower chemical valence of Zr cation in the present system. All the Zr 3*d* spectra can be well fitted (Figure 4). The Zr $3d_{5/2}$ spectra of both samples can be well fitted to the sum of two peaks. One is at 184.90 ± 0.15 eV and the other is at 183.80 ± 0.15 eV. By the comparison with the binding energy of the pure ZrF_4, the higher binding energy can be ascribed as the Zr^{4+} state, while the peak with the lower one is ascribed to the lower valance state of zirconium. Compared to the two Zr 3*d* spectra as shown in Figure 4, the ratio of the lower valance Zr increases with increasing content of Zr. The previous studies on yttrium stabilized zirconia (YSZ), which was exposed to a reducing environment (H_2) at 1273 K, also found the phenomenon of Zr 3*d* peaks broadened towards the lower binding energy.[23] The XPS spectra of YSZ showed a feature at lower binding energy for Zr 3*d* and without any changes in the XRD pattern, which also confirms that the reduction of the chemical valence state of Zr^{4+} cations occurs in the present solid solutions of $(Sc_{1-x}Zr_x)F_{3+\delta}$.

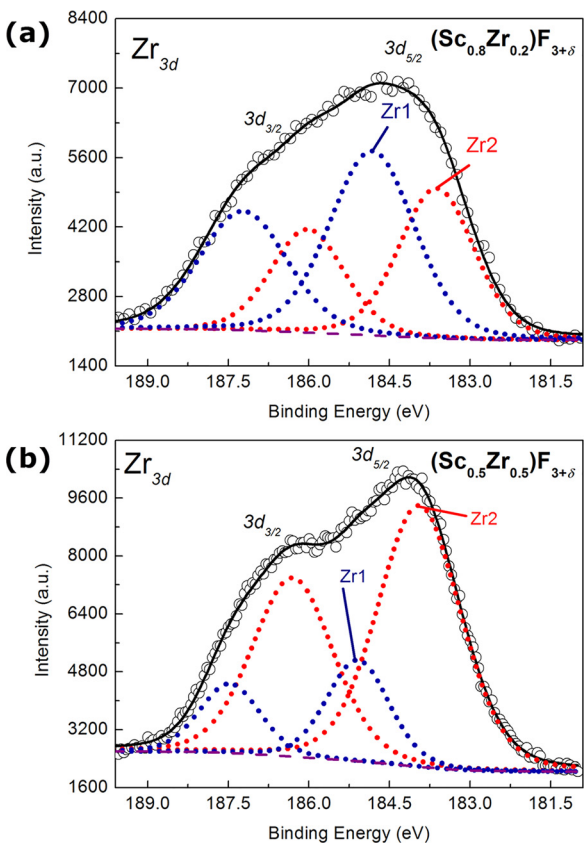

FIG. 4. Zr 3*d* XPS spectra of (a) $(Sc_{0.8}Zr_{0.2})F_{3+\delta}$ and (b) $(Sc_{0.5}Zr_{0.5})F_{3+\delta}$.

It should be noted that the stoichiometry of F ions of $(Sc_{1-x}Zr_x)F_{3+\delta}$ might deviate due to the chemical substitution of higher valence of Zr for Sc. Here, we introduce "δ" to present the stoichiometry deviation of F ions. It is known that Zr^{4+} does not have unpaired electrons. When the chemical valence states of Zr^{4+} drop, the subsequent emergence of unpaired electrons may contribute to the appearance of magnetic order. Manipulating the valance state of dopant ions is a possible method to tune the magnetic properties of the samples. Similar phenomenon has been obtained by Yan *et al.*, in which they introduced Mn^{2+} ions into the NiO host and doped Li^+ ions to influence the Mn^{2+}/Mn^{3+} ratio to further control the ferromagnetic property.[24]

In summary, controllable thermal expansion has been obtained by the chemical substitution of Sc with Zr in the ScF_3 based compounds. More interestingly, zero thermal expansion has been achieved in the composition of $(Sc_{0.8}Zr_{0.2})F_{3+\delta}$ over a wide temperature range (298 K–648 K). The room temperature magnetic order behavior has been found in $(Sc_{0.8}Zr_{0.2})F_{3+\delta}$, which presumably correlates closely with the lower chemical valence of Zr cation. This present result could be a good reference for designing multifunctional compounds with the controllable thermal expansion property.

See supplementary material for sample preparation, experimental methods, and data analysis procedures that are included.

This work was supported by the National Natural Science Foundation of China (Grant Nos. 21322102, 91422301, 21231001, 21590793, 51401224, and 51522705), National Program for Support of Top-notch Young Professionals, the Program for Changjiang Young Scholars, and the Fundamental Research Funds for the Central Universities, China (FRF-TP-14-012C1). The synchrotron radiation experiments were performed at the BL44B2 of Spring-8 with the approval of the Japan Synchrotron Radiation Research Institute (JASRI) (Proposal No. 2016A1060). This research used resources of the Advanced Photon Source, a U.S. Department of Energy (DOE) Office of Science User Facility operated for the DOE Office of Science by Argonne National Laboratory under Contract No. DE-AC02-06CH11357.

[1]J. Evans, P. Hanson, R. Ibberson, N. Duan, U. Kameswari, and A. Sleight, J. Am. Chem. Soc. **122**, 8694 (2000).
[2]J. Chen, L. Hu, J. Deng, and X. Xing, Chem. Soc. Rev. **44**, 3522 (2015).
[3]J. Chen, L. Fan, Y. Ren, Z. Pan, J. Deng, R. Yu, and X. Xing, Phys. Rev. Lett. **110**, 115901 (2013).
[4]P. Mohn, Nature **400**, 18 (1999).
[5]K. Takenaka and H. Takagi, Appl. Phys. Lett. **87**, 261902 (2005).
[6]M. Azuma, W. T. Chen, H. Seki, M. Czapski, K. Oka, M. Mizumaki, T. Watanuki, N. Ishimatsu, N. Kawamura, and S. Ishiwata, Nat. Commun. **2**, 347 (2011).

[7]T. A. Mary, J. S. O. Evans, T. Vogt, and A. W. Sleight, Science **272**(5258), 90 (1996).
[8]S. E. Tallentire, F. Child, I. Fall, L. Vella-Zarb, I. R. Evans, M. G. Tucker, D. A. Keen, C. Wilson, and J. S. Evans, J. Am. Chem. Soc. **135**, 12849 (2013).
[9]B. K. Greve, K. L. Martin, P. L. Lee, P. J. Chupas, K. W. Chapman, and A. P. Wilkinson, J. Am. Chem. Soc. **132**, 15496 (2010).
[10]L. Hu, J. Chen, A. Sanson, Y. Yang, and X. Xing, J. Am. Chem. Soc. **138**, 8320 (2016).
[11]M. P. Attfield and A. W. Sleight, Chem. Mater. **10**, 2013 (1998).
[12]X. Shen, C. Viney, E. R. Johnson, C. Wang, and J. Q. Lu, Nat. Chem. **5**, 1035 (2013).
[13]K. W. Chapman, P. J. Chupas, and C. J. Kepert, J. Am. Chem. Soc. **128**, 7009 (2006).
[14]C. R. Morelock, B. K. Greve, L. C. Gallington, K. W. Chapman, and A. P. Wilkinson, J. Appl. Phys. **114**, 213501 (2013).
[15]C. R. Morelock, L. C. Gallington, and A. P. Wilkinson, Chem. Mater. **26**, 1936 (2014).
[16]C. R. Morelock, L. C. Gallington, and A. P. Wilkinson, J. Solid State Chem. **222**, 96 (2015).
[17]S. U. Handunkanda, E. B. Curry, V. Voronov, A. H. Said, G. G. Guzman-Verri, R. T. Brierley, P. B. Littlewood, and J. N. Hancock, Phys. Rev. B **92**, 134101 (2015).
[18]R. D. Shannon, Acta Crystallogr., Sect. A: Cryst. Phys., Diffr., Theor. Gen. Crystallogr. **32**, 751 (1976).
[19]A. R. Denton and N. W. Ashcroft, Phys. Rev. A **43**, 3161 (1991).
[20]L. Hu, J. Chen, L. Fan, Y. Ren, Y. Rong, Z. Pan, J. Deng, R. Yu, and X. Xing, J. Am. Chem. Soc. **136**, 13566 (2014).
[21]F. Han, J. Chen, L. Hu, Y. Ren, Y. Rong, Z. Pan, J. Deng, and X. Xing, J. Am. Ceram. Soc. **99**, 2886 (2016).
[22]L. Hu, J. Chen, L. Fan, Y. Ren, Q. Huang, A. Sanson, Z. Jiang, M. Zhou, Y. Rong, and Y. Wang, Adv. Mater. **27**, 4592 (2015).
[23]M. B. Pomfret, C. Stoltz, B. Varughese, and R. A. Walker, Anal. Chem. **77**, 1791 (2005).
[24]W. Yan, Z. Sun, and Z. Li, Adv. Mater. **24**, 353 (2012).